

Title No. 120-M29

Tensile Creep of Metakaolin-Limestone Powder Ultra-High-Performance Concrete

by Rodolfo Bonetti, Oguzhan Bayrak, Kevin Folliard, and Thanos Drimalas

An investigation was performed on the drying shrinkage and tensile drying creep characteristics of a nonproprietary ultra-high-performance concrete (UHPC) mixture. The mixture was formulated using metakaolin as the supplementary cementitious material (SCM) and limestone powder as the mineral filler. Cylindrical specimens with dimensions of 52 x 400 mm (2.05 x 16 in.) were fabricated and loaded at 7 and 11 days from casting to various stress levels for 90 days. Additional specimens were fabricated from a proprietary mixture with a silica fume-ground quartz formulation to study the effects of mixture composition. Simultaneous free drying shrinkage measurements were recorded in accompanying specimens placed in the same room environment. Attention was given to the effect of the casting orientation, age at loading, and mixture composition on the drying shrinkage and drying creep behavior of the samples. These tests show that the metakaolin-limestone powder mixture has significantly lower drying shrinkage and specific drying creep than the silica fume-ground quartz mixture. Additionally, the age at loading influences primary creep behavior while not affecting secondary creep at the same stress level. It seems that fiber orientation plays a significant role in the drying creep behavior of UHPC and that cracked UHPC under constant tensile stress undergoes a significant amount of fiber slip.

Keywords: casting orientation; drying shrinkage; mixture composition; tensile creep; ultra-high-performance concrete (UHPC).

INTRODUCTION

Ultra-high-performance concrete (UHPC) is a cementitious composite offering strength and durability features that could potentially transform the precast concrete industry. Nevertheless, the widespread use of UHPC as a standalone material for shear resistance requires some critical knowledge about its long-term behavior in tension. Creep consists of additional deformations over time in excess of the initial strain at a constant level of stress. In cementitious materials, creep is the result of water movement (microdiffusion) between capillary and gel pores,¹ producing local debonding of the intertwined solid phase of the calcium-silicate-hydrate (C-S-H) gel. Total creep strains are the sum of basic creep, occurring under sealed conditions, and drying creep, occurring under conditions of exposure to the environment. Concurrent deformations (shrinkage) caused by water loss influence the total deformation under constant stress. Internal water loss produces autogenous shrinkage. The loss of water to the environment produces drying shrinkage. These deformations need to be subtracted from the total deformation to obtain basic or drying creep values, as required by each case.

Tensile creep of UHPC is one of those areas where very limited research has been published, in part because of the

complexities surrounding the required test methods. Another obstacle has been the lack of a broadly accepted framework for determining the full spectrum of tensile behaviors of the material. Although some of these difficulties persist, various researchers^{2,3} have contributed to this knowledge base, mainly studying the tensile creep behavior of proprietary mixtures that have silica fume as the main supplementary cementitious material (SCM), with or without ground quartz as the mineral filler.

Garas Yanni² conducted a multiscale investigation on the tensile creep of UHPC, observing that the drying tensile creep of UHPC is several times greater than its compressive creep at the same relative stress level and that the long-term creep behavior is greatly affected by the porosity of the fiber-matrix interface. The researcher favored the use of thermal treatment and proper consolidation of the material if intended for use as shear reinforcement in bridge girders. A tensile creep study by Switek³ proposed the hypothesis that the nonlinear viscoelasticity observed in tensile creep specimens tested at an early age is mainly caused by the internal moisture changes verified during the incipient hydration process.

The work presented in this paper focuses on several aspects not covered extensively in the current literature related to the tensile creep behavior of nontraditional, nonproprietary UHPC.

RESEARCH SIGNIFICANCE

The use of UHPC for shear resistance constitutes a logical path of application for the material due to its enhanced tensile strength and ductility in comparison with high-strength concrete. However, the long-term behavior in tension of this relatively novel material has not been addressed in detail, which is one of the issues causing some stagnation of the technology. Various aspects have been identified where gaps in the current literature still exist, such as the effects on tensile creep of the age at loading, mixture composition, casting/fiber orientation, and the creep behavior of cracked specimens. This paper provides some answers to these issues.

ACI Materials Journal, V. 120, No. 2, March 2023.

MS No. M-2022-144.R1, doi: 10.14359/51738492, received October 16, 2022, and reviewed under Institute publication policies. Copyright © 2023, American Concrete Institute. All rights reserved, including the making of copies unless permission is obtained from the copyright proprietors. Pertinent discussion including author's closure, if any, will be published ten months from this journal's date if the discussion is received within four months of the paper's print publication.

EXPERIMENTAL PROCEDURE

Creep frames

Various test setups have been proposed^{2,3} for the long-term tensile creep testing of concrete and UHPC, most of them consisting of a dead load-lever arm system with some similarities to the one proposed by Bissonnette and Pigeon⁴ for fiber-reinforced concretes. The moveable creep frames built for the purpose of this study are inspired by the work of Switek³ with the introduction of several modifications. These modifications were intended to increase stiffness and minimize out-of-plane deformations, and accommodate a lever arm ratio of 6:1 and bigger loading plates for the use of steel weights. Additionally, the frames were made in two sections to make possible their placement and assembly inside the controlled environment room. Figure 1 depicts the steel frames fabricated for this investigation. Calibration of each lever was performed prior to the use of the creep frames. This was achieved by applying incremental step loading at the tip of the lever and measuring the tensile force reaction through a donut load cell located at the top of the frame. The slope of the resulting straight line of the tensile force versus applied load was the value of the lever ratio. All the values of the lever ratio were found to be within $\pm 3\%$ of the theoretical value of 6.

Materials

A nonproprietary mixture was developed for this shrinkage and creep study, with metakaolin as the SCM at an amount of 30% of cement content by weight. Limestone powder was used as the mineral filler with an average particle size of 100 μm . Packing optimization of dry constituents was achieved by using the sum of squares of residuals (SSR) of the total grading curve points, departing from the modified Andreassen and Andersen model with a k -value of 0.225. An air detainer in a 1% dose by cement weight was added to the mixture to curb some of the entrapped air introduced by the high amount of high-range water-reducing admixture (HRWRA) required for workability. Table 1 shows the composition of the mixture described previously. The proprietary mixture used in this study has silica fume as the main SCM and ground quartz as the mineral filler (refer to

Graybeal⁵). The mixing of the materials was performed in a horizontal pan mixer in batches of 0.033 m^3 (1.1 ft^3) with a total mixing time of 13 minutes for the nonproprietary mixture and up to 45 minutes for the proprietary mixture.

Specimens

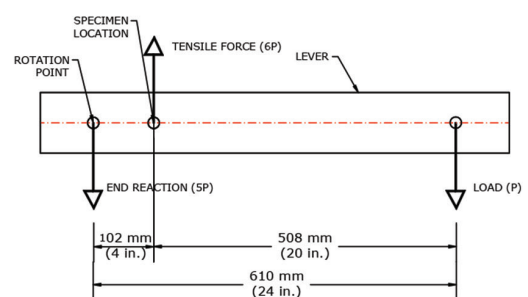
The creep specimens were cast in a casting bed, in clear, polyethylene terephthalate glycol (PETG) plastic tubes of 52 mm (2.05 in.) inside diameter and 1220 mm (48 in.) in length, using two different casting orientations intended to induce different preferential fiber alignment in the specimens. The first set of specimens was cast with the casting bed placed horizontally (0 degrees) and the second set with the casting bed in a vertical position (90 degrees). External vibration was used for the horizontal specimens to facilitate material placement. Figure 2 shows the casting orientations described previously. After casting, the tubes were sealed to prevent moisture loss and placed in an upright position until samples reached at least 55 MPa (8000 psi) of compressive strength, tested from accompanying 50 mm (2 in.) cubes. The specimens were then cut to 400 mm (16 in.) lengths using a concrete saw. Following cutting, the specimens were water cured for 3 additional days, after which their ends were slightly sanded, cleaned, and epoxied to receive the steel nipples that were attached to them.

Table 1—Nonproprietary mixture proportions

Material	Proportions by weight
Cement, PC Type V	1.000
Metakaolin	0.300
Limestone powder	0.523
Sand	1.400
Air detainer	0.010
HRWRA	0.051
Water	0.325
Steel fibers*	0.239

*Straight, 0.2 x 13 mm, 2% by volume.

Note: PC is portland cement.



PRINCIPLE OF OPERATION

Fig. 1—Overview of creep frames used in research.

Table 2—Summary of specimens in tensile creep test program

Specimen	Mixture	Casting orientation, degrees	Age at loading, days	Applied tensile stress, MPa (ksi)	Stress-strength ratio
L1	Nonproprietary	0	7	4.7 (0.68)	0.84
L2	Nonproprietary	0	7	4.7 (0.68)	0.84
L5	Nonproprietary	0	11	4.9 (0.71)	0.87
L6	Nonproprietary	0	11	4.1 (0.59)	0.72
L7	Proprietary	0	11	4.3 (0.63)	0.59
L9	Nonproprietary	90	11	3.7 (0.53)	0.85
L10	Nonproprietary	90	11	3.7 (0.53)	0.85

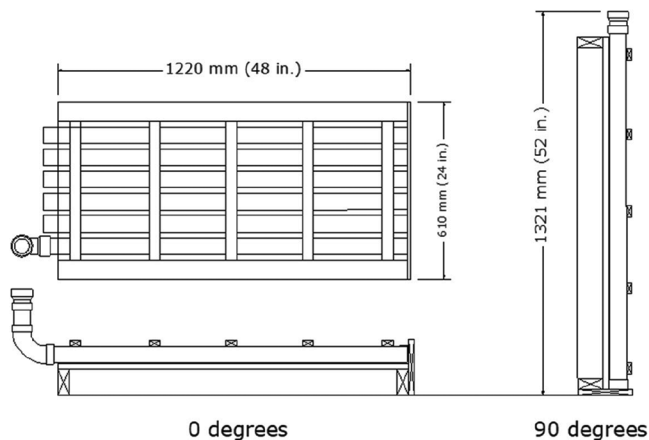


Fig. 2—Casting orientations for shrinkage and creep specimens.

The drying shrinkage specimens followed the same preparation procedure as the creep specimens, except that steel nipples were not attached to their ends. Figure 3(a) shows the shrinkage specimens resting on the free drying shrinkage table.

Instrumentation

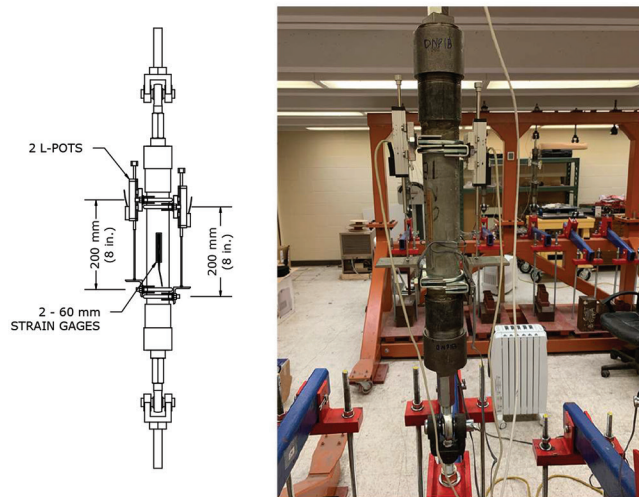
Two concrete surface strain gauges 60 mm (2.5 in.) long were glued to opposite sides of all the specimens. Additionally, the tensile creep specimens were instrumented with two 50 mm (2 in.) linear potentiometers located at 90 degrees from the strain gauges and at opposite sides of the specimens. The potentiometers were attached to the specimens with U-bolts, as shown in Fig. 3(b). All sensors were connected to a data acquisition system, and deformation values were recorded at a 5-minute time interval for the first 24 hours and at 30-minute increments afterward, until the end of the tests.

Loading procedure

The tensile strength of each mixture and casting direction was determined by direct tension tests prior to the loading of the creep specimens, as the average strength of two samples. The test method used to determine the tensile strength is a new direct tension test in displacement control at a loading rate of 0.15 mm/min (0.006 in./min).⁶ For the nonproprietary and proprietary mixtures cast at 0 degrees, the average tensile strengths were measured at 5.6 and 7.3 MPa (0.81 and 1.06 ksi), respectively. The tensile strength of the



(a) Shrinkage specimens



(b) Creep specimens

Fig. 3—Test setups for shrinkage and creep specimens.

nonproprietary mixture cast at 90 degrees was 4.3 MPa (0.62 ksi). These strength values served to determine the required amount of steel weights to place on the loading plates for each sample and depended on the target stress level. The calculation of these steel weights included the predetermined weights of hardware, lever, and plate. Table 2 shows the actual stress and stress-strength ratios applied to each of the samples. The specimens were attached and

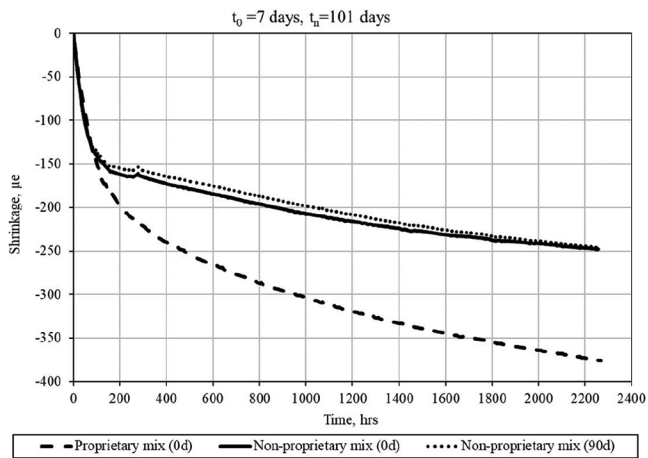


Fig. 4—Free drying shrinkage of proprietary and nonproprietary UHPC mixtures.

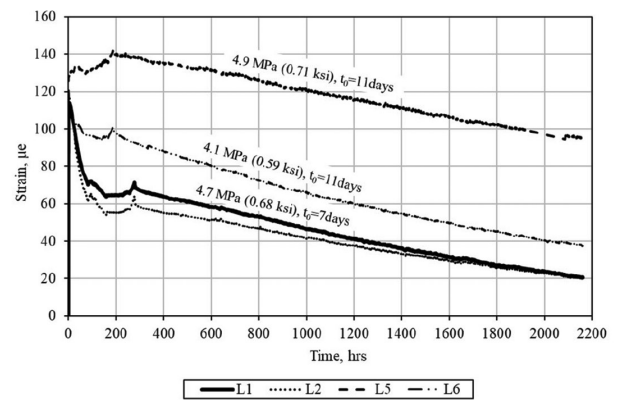
aligned to the frame and levers through two ball joints at each end. The load was progressively transferred to the specimens by simultaneously turning the nuts of the two hanging rods supporting the steel plates until the plates were approximately 38 mm (1.5 in.) above the bottom beams of the frames. The load-transfer operation lasted approximately 5 minutes. Additionally, temperature and humidity were controlled over the duration of the tests to $23 \pm 1^\circ\text{C}$ ($73 \pm 2^\circ\text{F}$) and $50 \pm 4\%$ relative humidity, respectively. Table 2 shows a summary of the creep specimens tested in this research program.

EXPERIMENTAL RESULTS AND DISCUSSION

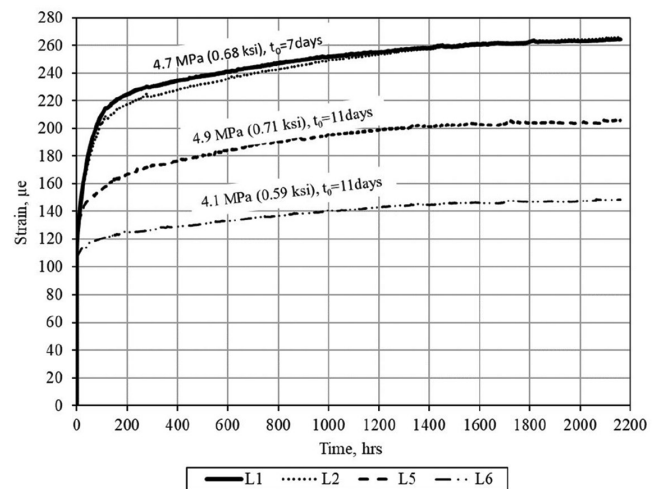
Drying shrinkage specimens

Drying shrinkage deformations from five specimens were recorded starting at 7 days of age and for 94 days afterward. The specimens rested over low-friction rods to prevent any restraint. Figure 4 shows the results of free drying shrinkage deformations as the average of two samples (two gauges each), except for the nonproprietary mixture cast vertically (90 degrees), where only the average of two gauges on one sample was measured. The experimental evidence shows the drying shrinkage behavior to be similar for both mixtures regardless of casting orientation for the first 100 hours, with a slightly steeper slope for the nonproprietary mixture. After this accelerated phase, shrinkage of the nonproprietary mixture progresses at a much lower rate than the proprietary mixture.

At 94 days of testing, the proprietary mixture drying shrinkage strains were 53% higher than those of the nonproprietary mixture. These results are somewhat unexpected because the nonproprietary mixture has a greater water-binder ratio (w/b) of 0.25 in comparison to the 0.20 ratio of the proprietary mixture. A plausible explanation for this behavior resides in the increased sand-powder ratio; a lower cement content; and larger particle size of the sand, mineral filler, and SCM (metakaolin) of the nonproprietary mixture. In terms of the preferential fiber orientation, it is apparent that casting orientation does not affect the drying shrinkage behavior of the nonproprietary mixture.



(a) Total strains specimens L1, L2, L5, L6 (0-deg cast orientation)



(b) Drying creep strains specimens L1, L2, L5, L6 (0-deg cast orientation)

Fig. 5—Total strains and drying creep of nonproprietary mixture (0-degree casting orientation).

Drying creep specimens

The 50 mm (2 in.) cube compressive strength and modulus of elasticity (ASTM C469) of the material at the time of load transfer were 124 MPa (18 ksi) and 41.4 GPa (6000 ksi), respectively. Drying creep deformations were calculated as the result of the total deformations minus the corresponding shrinkage deformations. Basic creep deformations in sealed specimens were not measured during this research because loading started at ages (7 and 11 days) where almost all autogenous shrinkage has taken effect in the specimens (refer to Fig. A.1 in Appendix A). Drying creep strains reported in Fig. 5(b) include the initial elastic strain, ϵ_o . Table A.1 in Appendix A shows the initial elastic deformation, ϵ_o , and the drying creep coefficient at 90 days (ϵ_{90}/ϵ_o) for the specimens in this research.

Effect of age at loading

Specimens L1 and L2 were loaded at 7 days from casting at a 4.7 MPa (0.68 ksi) stress level for 90 days. Specimens L5 and L6 were loaded at 11 days at stress levels of 4.9 MPa (0.71 ksi) and 4.1 MPa (0.59 ksi), respectively. Figures 5(a) and (b) show the total strains and drying creep strains for

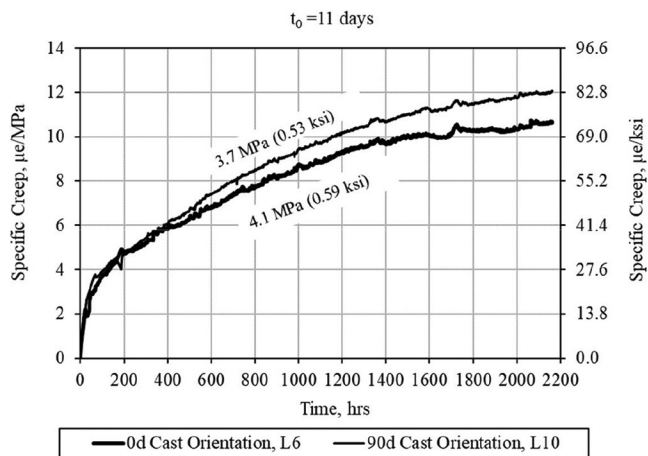


Fig. 6—Effect of casting orientation on specific drying creep of nonproprietary mixture.

these four specimens. It is evident that when specimens are loaded in tension at 7 days, the total strains are heavily affected by shrinkage in comparison to the lesser impact shown on those loaded at 11 days of age. Additionally, the age at loading affects the onset of the state of a constant rate of creep deformation (secondary creep). Specimens loaded at 11 days experienced a shortening of the primary creep stage in approximately 100 hours in comparison to those loaded at 7 days. Secondary creep seems to not be affected by the age at loading at approximately the same stress level. These findings are very similar to other results reported in the literature,^{3,7} tying a reduction in creep deformation to hydration evolution with time.

Effect of fiber orientation

Specimens L6 and L10 were loaded at 11 days of age at 4.1 and 3.7 MPa (0.59 and 0.53 ksi) stress levels, respectively. Specimen L6 was cast horizontally (0 degrees), whereas Specimen L10 was cast vertically (90 degrees). Specific drying creep for both specimens is presented in Fig. 6. These results show an increase in the specific creep of the specimen cast at 90 degrees in comparison to the specimen cast horizontally regardless of being loaded at a smaller stress level. This behavior could be explained by the microcracking effect theory (Neville et al.⁸ and Bissonnette et al.⁷). A preferential fiber orientation along the axis of the creep specimen, where the tensile stress is applied, will prevent the propagation of microcracks, thus reducing the potential total amount of creep in the specimen.

Effect of mixture composition

To study the effect of mixture composition, Specimen L7 from the proprietary mixture was loaded at 11 days of age at a 4.3 MPa (0.63 ksi) tensile stress level. This specimen was cast horizontally to produce a preferential fiber orientation along the longitudinal axis of the specimen. Drying specific creep values were obtained during the 90-day period of the creep tests and compared to those from Specimens L5 and L6 of the nonproprietary mixture, which had the same casting orientation. Results from these experiments (refer to Fig. 7) show an increase of specific creep for the proprietary

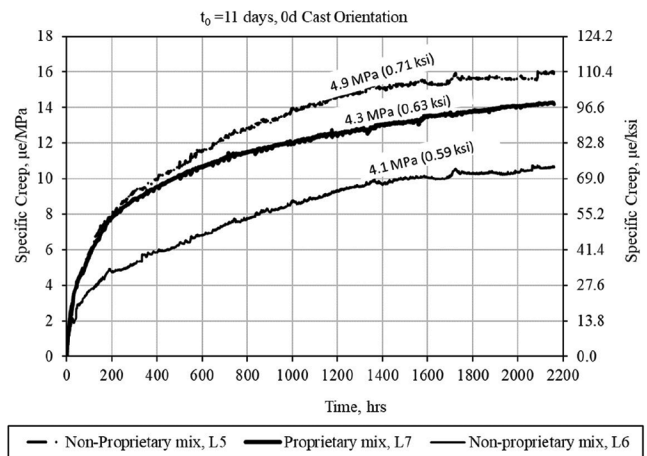


Fig. 7—Effect of mixture composition on specific drying creep.

mixture of 33% over the nonproprietary mixture at approximately the same stress level, and just 12% less specific creep than Specimen L5, which was loaded at a higher stress level of 4.9 MPa (0.71 ksi). Results by Garas Yanni² in untreated square section specimens, made of a proprietary mixture and tested at a stress level of 40% of tensile strength, show specific tensile creep of approximately five times greater than those shown in Table A.1 for the nonproprietary mixture tested at 7 days of age. A probable reason for this behavior resides in the finer raw materials and microstructure that is typically obtained from the silica fume-ground quartz mixtures that in turn produce an increase in both shrinkage and creep (refer to Fig. 4 and 7).

Creep of cracked specimens

Specimens L1, from the nonproprietary material, and L7, from the proprietary mixture, cracked during load transfer. However, results from this research suggest that there is no change in behavior for the uncracked portion of the material, as shown by a comparison of Specimens L1 (cracked) and L2 (uncracked), shown in Fig. 5(a) and (b). The position of the cracks was such that it permitted to record deformations with the linear potentiometers during the 90-day period of the creep tests (refer to Fig. 8). Results from these measurements indicate that right after cracking, the material starts experiencing fiber slip events in conjunction with drying creep. The fiber slip measured in the specimen made with the nonproprietary mixture (L1) was larger at transfer but experienced only one additional fiber slip event during the whole test period. Specimen L7, made with the proprietary mixture, experienced several fiber-slip events during the 90-day period of the test. These findings suggest that cracked UHPC elements in tension, under sustained loads, will experience a significant amount of fiber slip.

CONCLUSIONS

From the results of the tests in this investigation, the following conclusions can be drawn:

1. After 94 days of testing, the drying shrinkage of the silica fume-ground quartz (proprietary) mixture is 53%

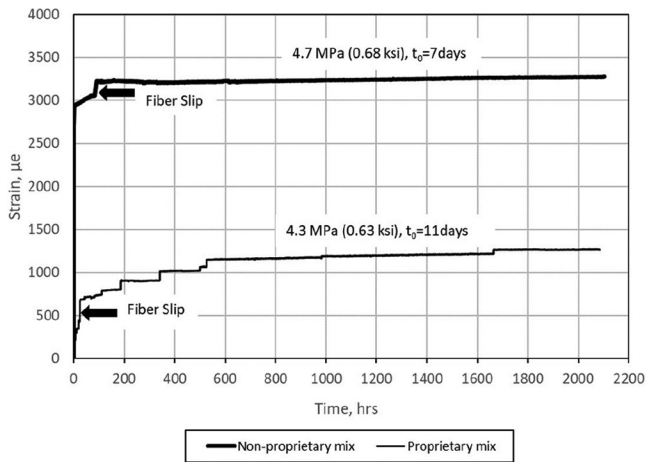


Fig. 8—Drying creep of cracked specimens.

greater than that of the metakaolin-limestone powder (nonproprietary) mixture.

2. The age at loading greatly affects primary creep but not secondary creep. After some progress in the hydration process, it seems that there are no significant changes in the viscoelastic properties of specimens loaded at 7 or 11 days of age at the same stress level.

3. Specific drying creep of the proprietary mixture is approximately 33% greater than that of the nonproprietary mixture at approximately a 4.1 MPa (0.6 ksi) stress level at 90 days.

4. Specific creep of 90-degree cast nonproprietary ultra-high-performance concrete (UHPC) is greater than the specific creep of 0-degree cast UHPC, even at a smaller stress level.

5. Recorded creep deformations of cracked specimens show a substantial amount of fiber slip at constant stress levels.

AUTHOR BIOS

ACI member **Rodolfo Bonetti** received his PhD in civil engineering from the University of Texas at Austin, Austin, TX, in 2022. He received his BS from Pontificia Universidad Católica Madre y Maestra, Santiago, Dominican Republic; and his MS from Virginia Tech, Blacksburg, VA. His research interests include the characterization of cementitious composites and the behavior of concrete structures.

Oguzhan Bayrak is the Phil M. Ferguson Professor in civil engineering at the University of Texas at Austin. His research interests include the

behavior, analysis, and design of reinforced and prestressed concrete structures; bridge engineering; evaluation of structures in distress; structural repair; fiber-reinforced polymers; and earthquake engineering.

Kevin Folliard is the Warren S. Bellows Centennial Professor in civil engineering at the University of Texas at Austin. His research interests include portland cement concrete, concrete durability, high-performance concrete, and controlled low-strength materials.

Thanos Drimalas is a Research Associate in the Department of Civil, Architectural and Environmental Engineering at the University of Texas at Austin, where he received his PhD in civil and environmental engineering in 2007. He is a member of ACI Committees 201, Durability of Concrete; 301, Specifications for Concrete Construction; 321, Concrete Durability Code; and 350C, Environmental Engineering Concrete Structure Code. His research interests include concrete durability and the use of supplementary cementitious materials (SCMs) in concrete.

ACKNOWLEDGMENTS

The authors are appreciative of Burgess, Huber Engineered Materials, Composites One LLC, Bekaert, and Sika USA for providing materials for this research.

NOTATION

t_0 = time at start of test (in days)
 t_n = time at end of test (in days)
 ϵ_o = initial elastic strain

REFERENCES

1. Bažant, Z. P., and Xi, Y., “Drying Creep of Concrete: Constitutive Model and New Experiments Separating Its Mechanisms,” *Materials and Structures*, V. 27, No. 1, Jan. 1994, pp. 3-14. doi: 10.1007/BF02472815
2. Garas Yanni, V. Y., “Multi-Scale Investigation of Tensile Creep of Ultra-High Performance Concrete for Bridge Applications,” PhD dissertation, Georgia Institute of Technology, Atlanta, GA, 2009, 291 pp.
3. Switek, A. E., “Time-Dependent Response of Ultra-High Performance Fibre Reinforced Concrete (UHPFRC) under Low to High Tensile Stresses,” PhD thesis, École Polytechnique Fédérale de Lausanne, Lausanne, Switzerland, 2011, 223 pp. doi: 10.5075/epfl-thesis-4899
4. Bissonnette, B., and Pigeon, M., “Tensile Creep at Early Ages of Ordinary, Silica Fume and Fiber Reinforced Concretes,” *Cement and Concrete Research*, V. 25, No. 5, July 1995, pp. 1075-1085.
5. Graybeal, B. A., “Material Property Characterization of Ultra-High Performance Concrete,” Report No. FHWA-HRT-06-103, Federal Highway Administration, Turner-Fairbank Highway Research Center, McLean, VA, 2006, 188 pp.
6. Bonetti, R.; Bayrak, O.; Folliard, K.; and Drimalas, T., “A Framework for Determining the Direct Tensile Properties of Ultra-High-Performance Concrete,” *ACI Materials Journal*, V. 120, No. 2, Mar. 2023, pp. 87-96. doi: 10.14359/51738374
7. Bissonnette, B.; Pigeon, M.; and Vaysburd, A. M., “Tensile Creep of Concrete: Study of Its Sensitivity to Basic Parameters,” *ACI Materials Journal*, V. 104, No. 4, July-Aug. 2007, pp. 360-368.
8. Neville, A. M.; Dilger, W. H.; and Brooks, J. J., *Creep of Plain and Structural Concrete*, Construction Press, London, UK, 1983, 361 pp.

APPENDIX A

Table A1—Summary of deformations in tensile creep specimens

Tensile creep specimens deformations summary				
Specimen name	Initial deformation ϵ_0 , $\mu\epsilon$	Final deformation Initial + Creep ϵ_{90} , $\mu\epsilon$	Specific creep at 90 days SC_{90} , $\mu\epsilon/\text{MPa}$ ($\mu\epsilon/\text{ksi}$)	Creep coefficient at 90 days Cr_{90}
L1	111	264	32.5 (225)	2.38
L2	111	266	33.0 (228)	2.40
L5	128	206	15.9 (110)	1.61
L6	106	149	10.6 (73)	1.41
L7	70	131	14.1 (97)	1.87
L9	91	141	13.6 (94)	1.55
L10	94	137	11.7 (81)	1.46

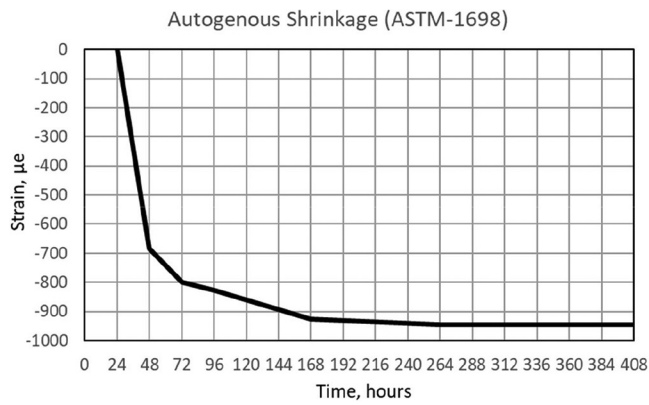


Fig. A1—Autogenous shrinkage of nonproprietary UHPC. (Note: Results shown are average of three samples.)

NOTES:
